LDI-MS Assisted by Chemical-Free Gold Nanoparticles: Enhanced Sensitivity and Reduced Background in the Low-Mass Region

ARTICLE *in* ANALYTICAL CHEMISTRY · NOVEMBER 2013

Impact Factor: 5.64 · DOI: 10.1021/ac401662r · Source: PubMed

3 AUTHORS:

Vincenzo Amendola
University of Padova
61 PUBLICATIONS **1,674** CITATIONS
SEE PROFILE

Lucio Litti
University of Padova
7 PUBLICATIONS **34** CITATIONS
SEE PROFILE

Moreno Meneghetti
University of Padova
151 PUBLICATIONS **3,836** CITATIONS
SEE PROFILE

analytical chemistry

Article

pubs.acs.org/ac

LDI-MS Assisted by Chemical-Free Gold Nanoparticles: Enhanced Sensitivity and Reduced Background in the Low-Mass Region

Vincenzo Amendola,* Lucio Litti, and Moreno Meneghetti

Department of Chemical Sciences, University of Padova, Via Marzolo 1, I-35131 Padova, Italy

Supporting Information

ABSTRACT: Gold nanoparticles (AuNPs) assisted laser desorption ionization mass spectrometry (LDI-MS) emerged as an effective technique for the detection of analytes with high sensitivity. The surface chemistry and the size of AuNPs are the crucial parameters for lowering the detection limits and increasing the selectivity of LDI-MS. Here we show that chemical-free size selected AuNPs, obtained by laser ablation synthesis in solution (LASiS), have very low background in the low mass region (<500 Da), contrary to citrate stabilized AuNPs (citrate-AuNPs) and dihydroxyacetophenone (DHAP). This allowed better performances for the picomole detection of low mass analytes like arginine, fructose, atrazine, anthracene and paclitaxel. The results suggest that chemical-free LASiS-AuNPs can be an excellent matrix for nanoparticle-assisted LDI-MS.

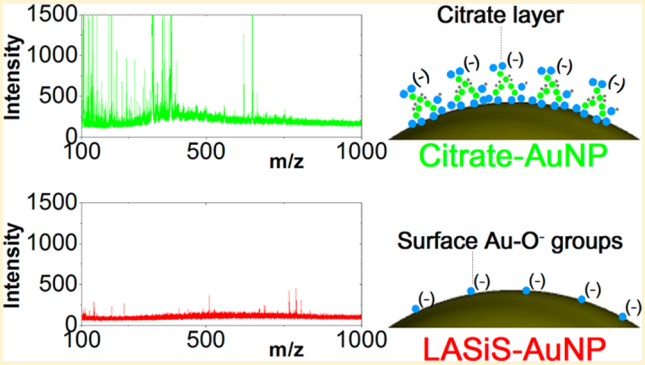

Laser desorption ionization mass spectrometry (LDI-MS) is a powerful technique for the detection of various analytes like peptides, polymers, proteins, carbohydrates, and lipids.[1,2] The desorption and ionization of analytes with mass above 500 m/z is often enhanced by an organic matrix (matrix-assisted LDI or MALDI) capable of efficient UV laser light absorption and preferential production of charged adducts between the analyte and ions from the matrix, usually protons.[3,4] However, LDI-MS analysis with organic matrixes may have problems of signal reproducibility and of chemical noise because of the production of cluster ions, which complicate mass spectra in the small molecular weight range (<800 m/z).[5,6] In addition, the inhomogeneous crystallization of organic matrix may affect signal reproducibility and linearity.[5,7,8]

In recent years, the use of gold nanoparticles (AuNPs) emerged as a valid alternative to organic matrixes for LDI-MS,[5,8] especially after the work of Russell's group.[6,9,10] AuNPs showed lower molar matrix-to-analyte ratio and higher shot to shot reproducibility than conventional organic matrixes,[5,6] as thoroughly discussed, for instance, by Cioffi et al.[5] and by Chang et al.[8] AuNPs have peculiar physical-chemical properties like low heat capacity[5] and intense absorption because of single electron interband transitions in the UV and surface plasmon resonance in the visible regions.[11] The plasmon absorption band is broadened and red-shifted when nanoparticles are agglomerated, for instance, by drying a drop of colloidal gold to form a substrate for LDI.[11,12] Therefore, visible laser pulses can be used for LDI of analytes that are subjected to rapid photodegradation by irradiation with UV pulses.[5,8,13,14]

Since AuNPs are chemically inert, sample preparation and deposition is greatly facilitated in many cases. For instance, AuNPs have high tolerance to chemical additives used in biological analysis, like surfactants,[5,13,15,16] which allows a great range of deposition conditions (pH, solvents),[10] and AuNPs matrixes can be stored for a long time in ambient conditions without degradation.[17,18] Most important, AuNPs are inert and biocompatible, thus they do not interfere with the stability of analytes and they are suitable for in vivo experiments.[6]

Analyte adsorption on the matrix is a crucial point of LDI-MS. AuNPs are especially suited for assisting LDI-MS because of their high specific area, viz., the surface area for unit mass, which implies an high extraction capacity.[5,6] The specific area depends linearly on nanoparticle size and, indeed, size dependent ion yield has been previously reported for LDI-MS of peptides by using AuNPs.[6] Also the surface temperature reached by laser irradiation increases with decreasing particle size.[8,19] Therefore, the use of size selected AuNPs must be a prerequisite for reproducible results and accurate comparison of LDI-MS performances with other types of nanomaterials and organic matrixes.

The surface chemistry of AuNPs is another factor strongly influencing the performances of LDI-MS.[5,10] It is worth to point out that to prevent aggregation, AuNPs from wet chemistry methods require stabilization with capping agents that are chemically (thiolated ligands) or physically (citrate molecules) bound to nanoparticles surface.[17] In several cases, the surface chemistry of AuNPs can be exploited for selective extraction and enrichment of a predetermined analyte.[5,9] For instance, by the Au−S chemical functionalization, the selective

Received: June 5, 2013
Accepted: November 6, 2013
Published: November 6, 2013

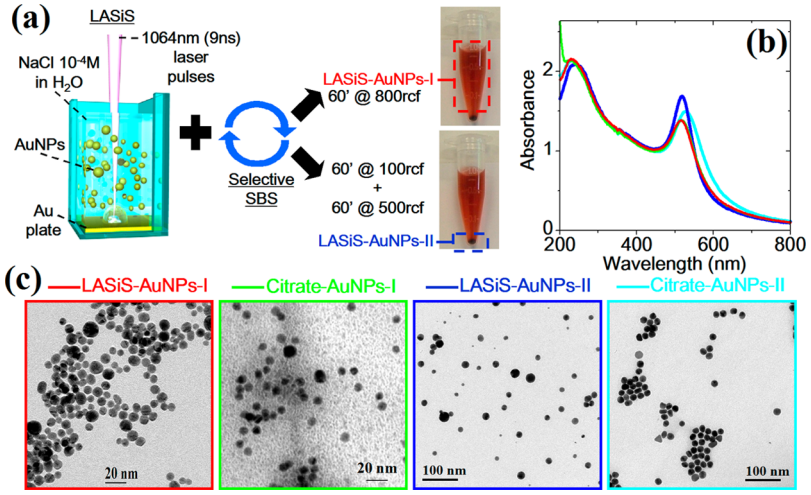

Figure 1. (a) Sketch of the preparation of size selected LASiS-AuNPs: AuNPs are formed by laser ablation with 1064 nm (9 ns) laser pulses of a bulk gold plate immersed in a NaCl 10^{-4} M solution in bidistilled water. Then, LASiS-AuNPs-I and -II are obtained by a selective SBS protocol with two different centrifugation speeds using a benchtop centrifuge. Optical absorption spectra (b) after the concentration/dialysis step and TEM images (c) of LASiS-AuNP-I (red line), LASiS-AuNP-II (blue line), citrate-AuNPs-I (green line), and citrate-AuNPs-II (magenta line).

targeting, capture and enhanced protonation of specific peptides and proteins was reported.[9,20,21] However, the targeting ligands generate mass peaks which may interfere with analyte signals or may yield to spectrum congestion in case of extensive fragmentation, hence small targeting molecules are usually preferred in order to limit these effects to the low mass range.[5] Analytes bearing specific functional groups like thiols,[22−24] amines,[5,8,22] disulfides,[5,8] and thioethers,[22,23,25] charged macromolecules like DNA[26] and neutral carbohydrates[25,27,28] can selectively bind the surface of bare AuNPs by chemical, physical, or electrostatic affinity.

Capping agents contribute significantly to the mass spectra, as various studies showed the sensitivity of AuNPs LDI-MS performances to the presence of passivating impurities.[10] In particular, because of the large amount of sodium citrate needed to stabilize citrate-AuNPs, LDI mass spectra contain multiple adducts, with concomitant spectra congestion and reduction of reference signals from $[M + H]^+$ and $[M + Na]^+$.[6,9] The availability of AuNPs devoid of the above limitations is a crucial requirement to improve the application range of LDI-MS. The ability to ionize chemical species with minimal chemical noise is especially relevant to biomarker detection or imaging MS, where the analysis often aims at the detection of low abundance analytes such as steroids or vitamins in complex mixtures.[29] Increasing the useful analyte mass range for LDI-MS by using exactly the same type of matrix would be important also for simultaneous analysis of multiple analytes in a wide mass interval.[5]

However, no reports investigated yet whether AuNPs obtained by laser ablation synthesis in solution (LASiS) have the potential to overcome the limitations of citrate-AuNPs for LDI-MS. In LASiS, AuNPs are produced by laser ablation of a bulk gold plate immersed in a liquid solution without chemicals or stabilizing molecules.[18] LASiS is compatible with the 12 principles of "green chemistry", it allows the production of milligrams of AuNPs in few minutes in a low-cost and reproducible way,[18,30,31] with a simple experimental set up requiring limited manual operation.[18,30,32,33] Indefinitely stable spherical AuNPs can be obtained in diluted NaCl solutions (10^{-4}−10^{-5} M) in pure water, without aggregation also at concentrations ∼20 times larger than commercial citrate-AuNPs,[18] and they are commercially available from several spin-off companies. Since the third (355 nm) or fourth (266 nm) harmonic of nanosecond Nd:YAG lasers are exploitable for LDI,[14] while the fundamental (1064 nm) of the same laser can be used for LASiS, in principle MALDI spectrometers can be designed for both nanoparticles preparation and MS analysis in the same laboratory, after a careful evaluation of safety requirements and cost-benefit ratio.

To date only few studies considered nanoparticles obtained by LASiS for LDI-MS of analytes. LASiS-AuNPs have been previously investigated by Tsuji et al. as interesting materials for the formation of clean LDI substrates.[34] LASiS-AuNPs are also promising for the preparation of impregnated porous alumina substrates[35−37] and for MS imaging, which requires the coating of a tissue section with a thin layer of nanoparticles.[38] The performances of Cu, Ag, Au and Pt nanoparticles obtained by LASiS in water have been compared, showing that only AuNPs and PtNPs produced appreciable signals.[39] Since nanoscale Cu and Ag materials are coated by an oxide layer, while Au and Pt nanoparticles are not subjected to extensive surface oxidation, these results confirmed the crucial role of the surface chemistry for LDI-MS.[39] Importantly, small (5−10 nm) Pt nanoparticles performed better than large (20 nm) AuNPs,[39] in agreement with the previous findings of Russell's group about citrate-AuNPs,[6] and with a similar study about Pt nanoparticles (PtNPs) obtained in aqueous solutions.[40]

However, AuNPs obtained by LASiS with nanosecond laser pulses in pure water usually have standard deviation of 50−100%,[11,18,39−42] while size selected nanoparticles can be obtained only by postsynthesis processes like laser irradiation[43,44] or centrifugation.[44] LASiS-NPs considered in ref 39 and 40 were not size selected and authors observed partial agglomeration in several samples,[39,40] while citrate stabilized AuNPs have monodispersed well-defined size and negligible agglomeration. Importantly, no systematic comparison between the performances of nanoparticles obtained by LASiS or by chemical reduction was carried out in the low mass range to date, in order to investigate the effect of the different surface chemistry on MALDI-MS performances.

The critical and precise comparison of LDI-MS analysis assisted by LASiS-AuNPs or citrate-AuNPs is a stringent

dx.doi.org/10.1021/ac401662r | Anal. Chem. 2013, 85, 11747−11754

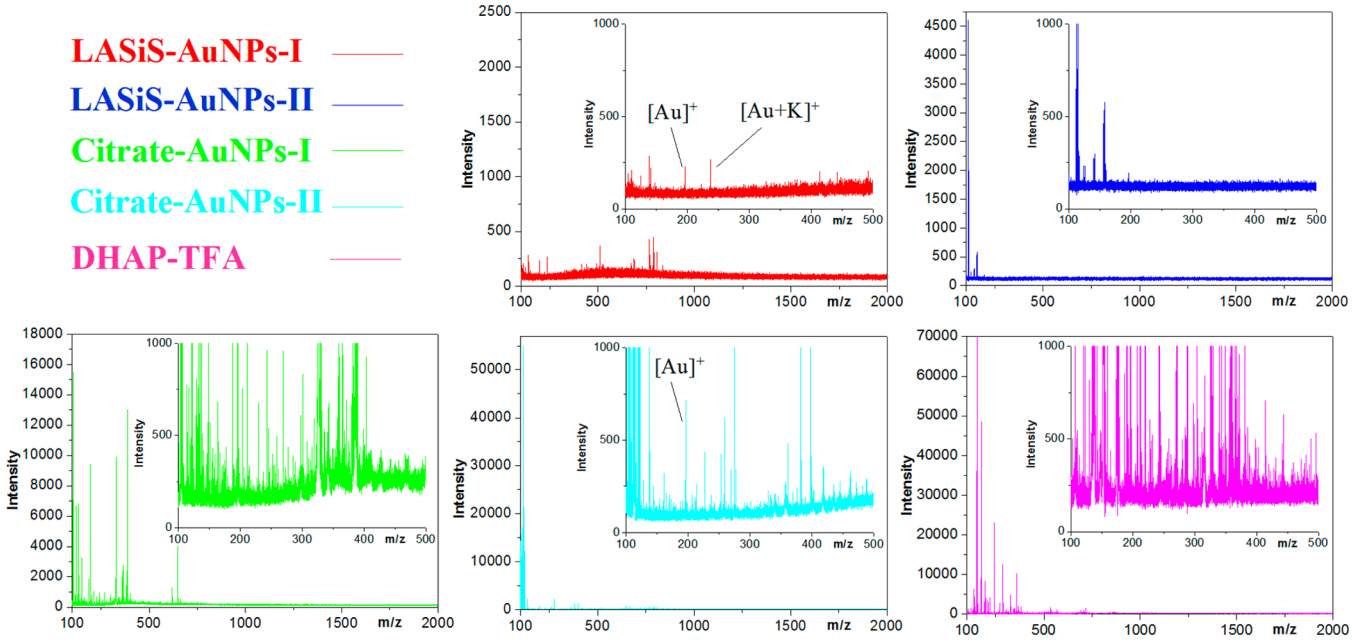

Figure 2. LDI-MS spectra of bare LASiS-AuNPs-I (red) and -II (blue), citrate-AuNPs-I (green) and -II (cyan) and DHAP-TFA (magenta). Inset shows a magnification of the low mass region.

requirement to asses what type of nanomaterials allows the best performances and deserves widespread application for this analysis.

Here we present the comparative study between the LDI-MS performances of size selected chemical free LASiS-AuNPs and of commercial citrate-AuNPs. LASiS-AuNPs systematically yield negligible background in the low mass region, intended both as a lower level of chemical noise and a lower number of detected signals which are unrelated to analyzed sample. This allowed the analysis of molecules of analytical interest and low mass that are located in a range usually not exploitable with standard organic matrixes. The absence of stabilizers in LASiS-AuNPs marked the difference with citrate-AuNPs, suggesting that chemical-free LASiS-AuNPs are excellent candidates for nanoparticle assisted LDI-MS.

EXPERIMENTAL SECTION

Nanoparticles Preparation. AuNPs were obtained by laser ablation synthesis in solution (LASiS),[18,30,42] as described in Electronic Supporting Information (ESI) and sketched in Figure 1a. AuNPs obtained by LASiS in NaCl solution possess a negative charge because of the reaction of a small fraction of surface Au atoms (about 6%) with O and Cl atoms,[18,45,46] therefore, no other stabilizing molecules are required to maintain the colloidal solution indefinitely stable.[18]

Size selection of AuNPs was carried out by a selective sedimentation based separation (SBS) protocol adapted from ref 47., and two fractions were selected, respectively LASiS-AuNPs-I and LASiS-AuNPs-II, as described in Supporting Information and sketched in Figure 1a.

Citrate stabilized AuNPs in water with average size of either 10 (citrate-AuNPs-I) and 20 nm (citrate-AuNPs-II) were purchased from Sigma Aldrich (G1527) and BBInternational (EM.GC20) respectively.

All nanoparticles dispersions were prepared at the same Au atoms concentration of 0.013 ± 0.001 M (2.6 ± 0.2 mg/mL), corresponding to AuNPs concentration of 2.1×10^{-7}, 2.1×10^{-7}, 3.2×10^{-8}, and 2.6×10^{-8} M for LASiS-AuNPs-I, citrate-AuNPs-I, LASiS-AuNPs-II, and citrate-AuNPs-II, respectively. The concentration was evaluated by optical absorption spectroscopy according to the protocol described in ref 11. Average size and relative standard deviation of the four AuNPs samples are 10.6 nm ± 22% for the LASiS-AuNPs-I sample, 18.6 nm ± 35% for the LASiS-AuNPs-II sample, 10.2 nm ± 12% for the citrate-AuNPs-I sample and 19.6 nm ± 8% for the citrate-AuNPs-II sample (see Supporting Information Table S1).

MALDI Samples and Analysis. L-Arginine (200 ng/μL in water), D(−)fructose (200 ng/μL in water), atrazine (50 ng/μL in methanol:water 1:1), anthracene (350 ng/μL in methanol:water 2:1), and paclitaxel (115 ng/μL in methanol:water 1:1) from Sigma-Aldrich were used. We used dihydroxyacetophenone (DHAP, 40 mg/mL) in acetonitrile and trifluoroacetic acid (TFA, 0.1%) as a reference organic matrix. The analyte and matrix deposition methods, the analyte to matrix ratios and further experimental details are described in additional experimental methods and in Tables S1 and S2 in Supporting Information.

RESULTS

Optical absorption spectroscopy (Figure 1b) shows that AuNPs solutions are stable and not aggregated, since a sharp plasmon band in proximity of 520 nm is observed in all cases and no plasmonic absorption is found at longer wavelengths.[11] TEM images (Figure 1c) confirm that citrate-AuNPs-I and LASiS-AuNPs-I have nearly the same average size (see also Supporting Information Table S1 for average size and standard deviation). Importantly, the standard deviation on average size of LASiS-AuNPs-I and -II (Supporting Information Table S1 and Figure 1c) is much smaller than in all the previous studies.[34,39,40] In this way, for the first time, the effects of nanoparticle surface chemistry and of nanoparticle size on the MALDI performances can be easily discriminated and, hence, the reliable comparison of LASiS and citrate-AuNPs is possible.

dx.doi.org/10.1021/ac401662r | Anal. Chem. 2013, 85, 11747−11754

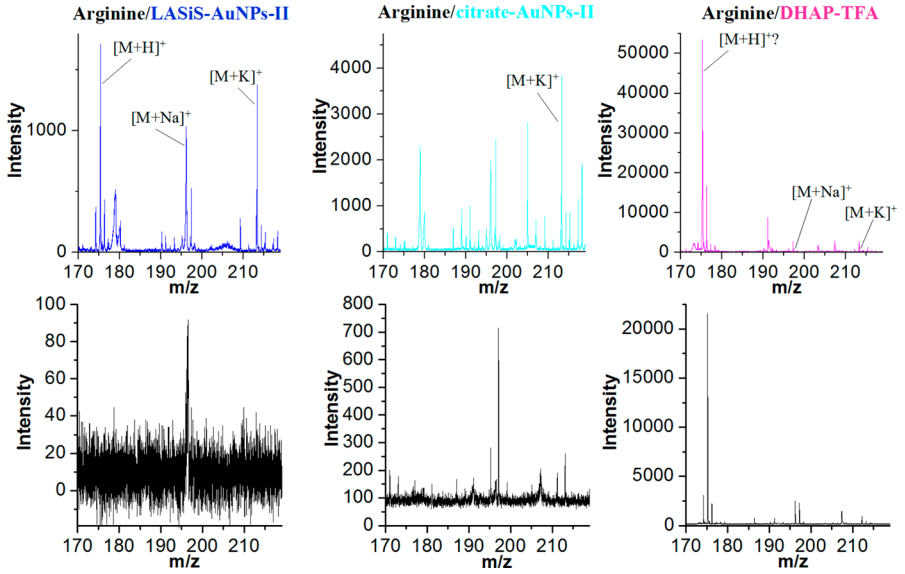

Figure 3. LDI-MS spectra of L-arginine assisted by LASiS-AuNP-II (blue), citrate-AuNP-II (cyan) or DHAP-TFA (magenta) matrixes. Below each plot, the spectra of the bare matrix is shown for comparison.

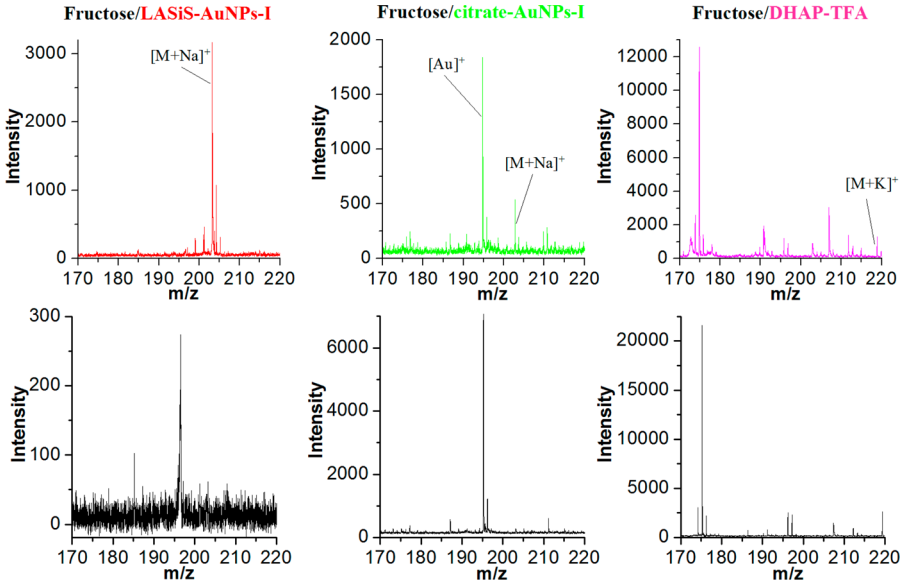

Figure 4. LDI-MS spectra of D(−)fructose assisted by LASiS-AuNP-I (red), citrate-AuNP-I (green), or DHAP-TFA (magenta) matrixes. Below each plot, the spectra of the bare matrix is shown for comparison.

As a first step, the mass spectra of the pure matrixes were collected and compared (Figure 2). A remarkable lower background (in absolute intensity) is observed below 800 *m*/*z* in LASiS-AuNPs, while spectrum congestion characterizes both citrate-AuNPs and the organic DHAP matrixes. The $[Au]^+$ and $[K+Au]^+$ ions are detected in the spectra of LASiS-AuNPs-I and citrate-AuNPs-II, while spectrum congestion does not allow the clear identification of peaks in citrate-AuNPs-I spectra.

Such a feature makes LASiS-AuNPs interesting for detection of analytes with mass below 500 *m*/*z*, that is, in the critical range usually not exploitable with this technique. Hence, we tested the LDI performances of all the five different matrixes for the detection of low mass analytes with different molecular structure (see Supporting Information Table S1) like arginine (a polar aminoacid), fructose (a small natural monosaccharide), atrazine (a polar molecule with aromatic groups widely used as herbicide), and anthracene (an apolar aromatic molecule). In the following, we report the best result among LASiS-AuNPs-I and -II, compared with the best one among citrate-AuNPs-I and -II and with the organic matrix.

In Figure 3, the LDI spectra of arginine collected on LASiS-AuNPs-II (blue), citrate-AuNPs-II (cyan) and DHAP-TFA (magenta) matrixes are reported. The mass spectra collected on the pure matrixes are shown below each graph for comparison. With LASiS-AuNPs, the most intense peaks in the arginine mass range are those of the $[M + H]^+$ (175.29 *m*/*z*), $[M + Na]^+$ (196.10 *m*/*z*) and $[M + K]^+$ (213.29 *m*/*z*) adducts. One peak at mass $[M + Na]^+$ (196.50 *m*/*z*) is found in the spectrum of the bare LASiS-AuNPs-II matrix, but 15 times less intense. The best spectrum collected with citrate-AuNPs matrix is crowded, since one peak assignable to $[M + K]^+$ (213.19 *m*/*z*) is observed together with several other peaks, also with larger intensity, whose identification is not straightforward. Appa-

dx.doi.org/10.1021/ac401662r | *Anal. Chem.* 2013, 85, 11747−11754

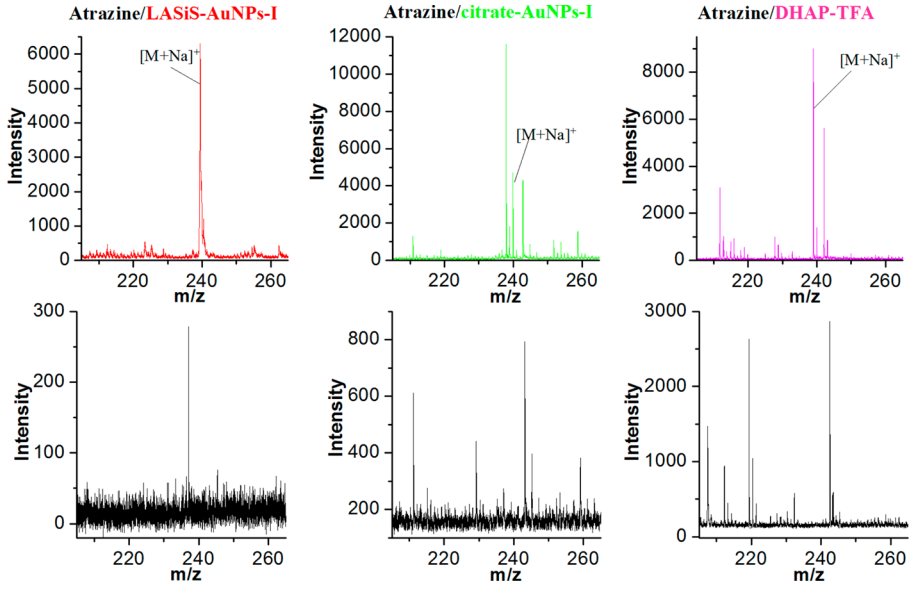

Figure 5. LDI-MS spectra of atrazine assisted by LASiS-AuNP-I (red), citrate-AuNP-I (green), or DHAP-TFA (magenta) matrixes. Below each plot, the spectra of the bare matrix is shown for comparison.

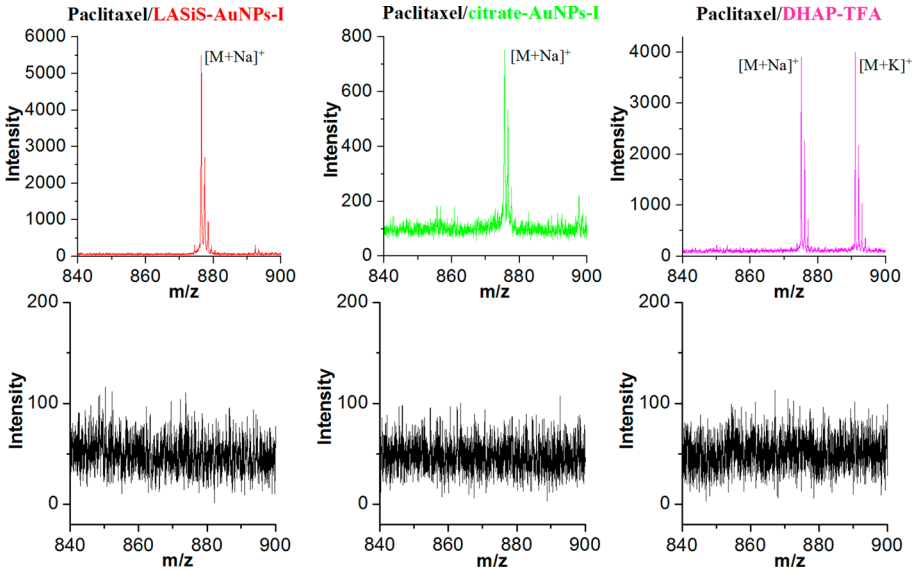

Figure 6. LDI-MS spectra of paclitaxel assisted by LASiS-AuNP-I (red), citrate-AuNP-I (green), or DHAP-TFA (magenta) matrixes. Below each plot, the spectra of the bare matrix is shown for comparison.

rently, the best spectrum collected with DHAP-TFA matrix shows a very intense peak at $[M + H]^+$ mass (175.25 m/z) and other peaks with lower intensity at $[M + Na]^+$ (197.25 m/z) and $[M + K]^+$ (213.25 m/z), but all these peaks are found also in the spectrum of the bare matrix, with comparably high intensity (175.22, 196.23, and 212.22 m/z, respectively), hence their assignment to the analyte would not be trustworthy.

The LDI mass spectra of fructose assisted by the three different types of matrixes is reported in Figure 4. The spectrum of fructose with LASiS-AuNPs matrix is dominated by the analyte peak at $[M + Na]^+$ mass (203.24 m/z), with negligible interference from the matrix. The $[M + Na]^+$ (202.79 m/z) peak is observed also in the spectrum collected with citrate-AuNPs matrix, although with low intensity, in fact the spectrum is dominated by the matrix peak at 194.78 m/z. With DHAP-TFA matrix, apparently the $[M + K]^+$ peak (218.85 m/z) is observed together with various peaks due to matrix background. Indeed, in the bare DHAP-TFA matrix spectrum there is another peak at the same mass of $[M + K]^+$ (219.32 m/z) and with similar intensity, hence no peaks can be reliably assigned to the analyte.

In Figure 5 we reported the best LDI-MS spectra of atrazine obtained with the three types of matrixes. With LASiS-AuNPs matrix, the $[M + Na]^+$ peak (239.43 m/z) is the only peak in the mass range of interest for atrazine. With citrate-AuNPs, multiple peaks close to the $[M + Na]^+$ mass are observed, likely due to analyte fragmentation. The peak with $[M+Na]^+$ mass (239.92 m/z) is the only one that can be easily assigned to atrazine, but the intensity is lower than with LASiS-AuNPs-I matrix. An intense signal at $[M + Na]^+$ mass (238.99 m/z) dominates the spectrum collected with the DHAP-TFA matrix, although there are several other peaks in part due to the matrix and in part possibly due to fragments of the analyte.

dx.doi.org/10.1021/ac401662r | *Anal. Chem.* 2013, 85, 11747−11754

The LDI-MS of anthracene with LASiS-AuNPs matrix yields only the $[M]^+$ (178.16 m/z) signal (Supporting Information Figure S1), while with citrate-AuNPs the spectrum is rich of peaks from the matrix close to the $[M + Na]^+$ signal (201.22 m/z). No $[M]^+$, $[M + H]^+$, $[M + Na]^+$, or $[M + K]^+$ peaks are found with the DHAP-TFA matrix, although a new signal is found close to 191 m/z that is not present in the matrix background and may be the result of analyte fragmentation.

Finally, we compared the performances of the five matrixes for the LDI-MS of paclitaxel, that is a widespread anticancer drug belonging to the category of taxanes. Paclitaxel mass (853.91 Da) is outside the critical range of MALDI, in fact no appreciable background is observed (Figure 6). The most intense and clean spectrum is obtained by LASiS-AuNPs-I, where only the Na adducts $[M + Na]^+$ (876.42 m/z) is present. The $[M + Na]^+$ peak is detected also with citrate-AuNPs matrix (875.61 m/z), but with remarkably lower intensity. With DHAP-TFA, both sodium ($[M + Na]^+$, 875.03 m/z) and potassium ($[M+K]^+$, 890.98 m/z) adducts are found, with lower intensity than with the LASiS-AuNPs matrix.

Interestingly, LASiS-AuNPs-I matrix performed better in terms of point-to-point signal reproducibility and linearity of the $[M + Na]^+$ peak intensity versus analyte concentration (red squares in Figure 7). The signals obtained with the citrate-AuNPs-I matrix also show a good linearity (green circles in Figure 7), although with lower signal intensity and lower correlation coefficient (R^2) than LASiS-AuNPs-I. On the opposite, we found that analyte signals do not scale linearly with analyte concentration when the DHAP-TFA matrix is used (magenta triangles in Figure 7).

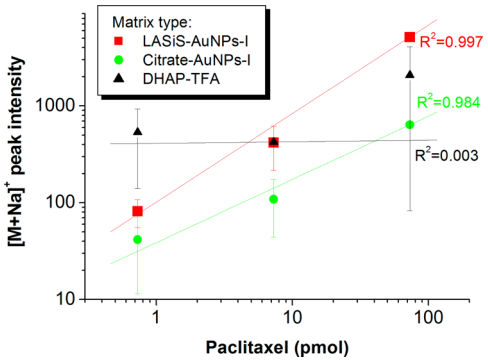

Figure 7. Log–log LDI-MS intensity plot of the $[M + Na]^+$ peak versus the pmol of paclitaxel deposed on the three different matrixes: LASiS-AuNP-I (red squares), citrate-AuNP-I (green circles), and DHAP-TFA (black triangles). Linear fit are reported as red, green, and black lines for LASiS-AuNP-I, citrate-AuNP-I, and DHAP-TFA, respectively. Error bars represent the standard deviation over three measurements.

DISCUSSION

When LASiS-AuNPs matrix is used, a remarkably low background and the absence of spectrum congestion is observed in the whole mass range, even below 500 m/z, contrary to citrate-AuNPs and DHAP-TFA matrixes (see also Supporting Information Figure S2). Consequently, the base peak comes from the analyte in the mass spectrum collected with LASiS-AuNPs matrix, while it is often due to matrix background or unidentified species when citrate-AuNPs or DHAP-TFA matrixes are used.

The experimental results are explained with the different surface chemistry of LASiS and citrate-AuNPs. Citrate-AuNPs are stabilized by a layer of citrate molecules physically adsorbed on nanoparticle surface (Figure 8a). For instance, commercial 10 nm citrate-stabilized AuNPs solution contains <0.04% sodium citrate, <0.01% tannic acid, and 0.02% sodium azide, as by the manufacturer specification sheet. Before the concentration step with dialysis membranes (see Experimental Section), the presence of stabilizers is very evident in the optical absorption spectrum of 10 nm citrate-AuNPs as an intense absorption in the 200–250 nm range (Figure 8b). As shown in Figure 1b, this absorption is sensibly reduced after the concentration step with dialysis membranes, but a fraction of citrate molecules must still be present on nanoparticle surface to maintain the stability of the colloidal system.

Differently, LASiS-AuNPs are obtained in a 10^{-4} M NaCl solution in bidistilled water, and they are stabilized by a negative charge due to the reaction of a small fraction of surface Au atoms (about 6%) with O and Cl atoms (Figure 8a);[18,45,46] therefore, no other molecules are physically or chemically bonded to nanoparticles' surface.[18] The optical absorption spectra of AuNPs as obtained by LASiS, namely before the size selection and concentration steps, correspond to that of bare gold nanoparticles and only the interband transitions of gold are observed in the 200–250 nm range (Figure 8b).[11,12]

Once dried on the stainless steel MALDI plate, the citrate-AuNPs will be coated by a thin layer of organic stabilizers (Figure 8c). Hence, background signals in the low mass region of spectra collected with citrate-AuNPs are likely originated by

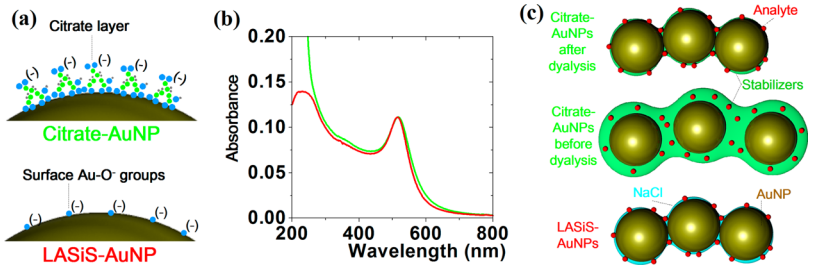

Figure 8. Sketch resuming the main difference between citrate and LASiS-AuNPs when they are in solution (a, b) or spotted on the stainless steel LDI plate (c). (a) In liquid solution, the surface of citrate-AuNPs is uniformly coated by a layer of negatively charged citrate ions, while the surface of LASiS-AuNPs is partially (~6%) oxidized and hosts Au–O^- groups without other stabilizing molecules. (b) The absorption spectrum of 10 nm citrate-AuNPs as obtained by the manufacturer shows a sharp absorption band in the 200–250 nm range, due to stabilizers, which is absent in the spectrum of AuNP as obtained by LASiS in 10^{-4} M NaCl solution in H_2O. (c) Once spotted on a substrate, the citrate-AuNPs are still coated by a layer of stabilizers, which can be thick if particles have not been dyalysed, while LASiS-AuNPs are coated by a layer of NaCl.

dx.doi.org/10.1021/ac401662r | Anal. Chem. 2013, 85, 11747–11754

the stabilizing molecules, which are fragmented by the laser desorption process and may form multiple adducts with the analyte, yielding spectrum congestion. We further confirmed that stabilizers are responsible for spectrum congestion at low mass in citrate-AuNPs by the LDI-MS spectra of the liquid contained in commercial citrate-AuNPs (Supporting Information Figure S3a), which was collected by dialysis, mixed with the LASiS-AuNPs-I sample and, finally, spotted on the stainless steel plate for MS analysis. As shown in Supporting Information Figure S3b, the "clean" LDI-MS spectrum of bare LASiS-AuNPs-I dramatically changed after mixing with the citrate-containing liquid, showing the appearance of several peaks with remarkably high intensity in the 100−600 m/z range (Supporting Information Figure S3b). Citrate molecules, because of their reducing power, may also interfere with the formation of cationic species, playing as a reducing agent.

It is worth to point out that, in our experiments, citrate-AuNPs were concentrated by dialysis, hence a large fraction of excess stabilizers was removed and the experimental conditions were the most favorable to the analysis. In pristine (i.e., not dialyzed) citrate-AuNPs, the stabilizers/AuNPs ratio is larger, hence the ligands' layer surrounding nanoparticles spotted on the stainless steel plate for LDI would be thicker than in dialyzed AuNPs (Figure 8c); consequently, this would further increase the probability of interaction between analytes and ligands' fragments and the intensity of low mass peaks due to ligands.

As synthesized LASiS-AuNPs are not coated by a stabilizing layer of molecules and the solution contains only a low amount of NaCl, therefore the proximity of the analyte with AuNPs is favored in comparison to the citrate-AuNPs and we have not identified any strong peak ascribable to adducts between the analyte and surface O or Cl atoms, hence there are no species which can originate large background and spectrum congestion (Figure 8c).

Since the synthesis of LASiS-AuNPs takes place in aqueous solution of NaCl and no proton donating species are present, the formation of analyte-sodium adducts is largely favored with this matrix and, indeed, this is observed in all cases except anthracene. We also found larger signals with polar analytes like arginine, fructose, atrazine and paclitaxel than with anthracene (the only nonpolar analyte), which can be explained with the lower tendency of the nonpolar molecules to form sodium adducts. This is in agreement with the fact that MALDI performances are improved when matrix and analyte polarity match.[48]

Also with citrate-AuNPs matrix, due to the presence of sodium citrate, sodium adducts often are the dominating analyte peaks. Evidently, sodium citrate and the other stabilizers favor the formation of sodium adducts instead of proton adducts. We know from literature[28] that the intensity of peaks due to sodium adducts may increase with Na^+ concentration in the sample, and we know from the product specification sheet of commercial citrate-AuNPs-I that Na^+ concentration is of the order of 6×10^{-3} M, while the concentration of the same cation in the LASiS-AuNPs-I sample is 1×10^{-4} M, hence we can conclude that the observed superiority of LASiS-AuNPs compared to citrate-AuNPs can not be ascribed to the concentration of Na^+ ions.

In our experimental conditions, no specific trends were observed with the analyte deposition method (i.e., premixed or sequential deposition). We found a similar trend between samples I and II of LASiS-AuNPs, as well as between samples I and II of citrate-AuNPs, although smaller particles (i.e., samples I) generally yielded better signals, in agreement with previous observations of Russell's group[6] and with the trend generally observed in literature.[5,8] However, by the comparison of mass spectra collected on LASiS-AuNPs-II and citrate-AuNPs-I, emerged that LASiS-AuNPs-II (average size 18.6 nm) performed better than citrate-AuNPs-I (average size of 10.2 nm) for the detection of arginine, fructose, and paclitaxel. This suggests that the difference in surface chemistry between LASiS-AuNPs and citrate-AuNPs has a stronger influence on the MALDI-MS performances than the difference in average size between LASiS-AuNPs-I and -II or between citrate-AuNPs-I and -II.

CONCLUSIONS

We compared the LDI-MS performances of size selected chemical free LASiS-AuNP and of commercial citrate-AuNPs and DHAP−TFA organic matrix. LASiS-AuNPs systematically give negligible background and no spectrum congestion in the low mass region (below 500 m/z) and are suitable for the analysis of low molecular weight species. Picomoles of arginine, fructose, atrazine, anthracene, and paclitaxel were successfully detected with LASiS-AuNPs matrix. LASiS-AuNPs also showed the best linearity versus analyte concentration. The absence of stabilizers in LASiS-AuNPs marked the difference with citrate-AuNPs, suggesting that chemical-free LASiS-AuNPs are excellent candidates for nanoparticle assisted LDI-MS.

ASSOCIATED CONTENT

Supporting Information

Additional experimental details, matrixes and analyte data, and LDI-MS spectra. This material is available free of charge via the Internet at http://pubs.acs.org.

AUTHOR INFORMATION

Corresponding Author

*E-mail: vincenzo.amendola@unipd.it.

Notes

The authors declare no competing financial interest.

ACKNOWLEDGMENTS

C. Zonta, D. Russell, and R. Gamez are gratefully acknowledged for useful discussions and support to this research. We thank Dr. G. Toffoli and Dr. E. Marangon for providing paclitaxel. We acknowledge University of Padova grant (PRAT) no. CPDA114097/11 and AIRC 5 × 1000 grant "Application of Advanced Nanotechnology in the Development of Innovative Cancer Diagnostics Tools".

REFERENCES

(1) Tanaka, K.; Waki, H.; Ido, Y.; Akita, S.; Yoshida, Y.; Yoshida, T.; Matsuo, T. *Rapid Commun. Mass Spectrom.* **1988**, *8*, 151−153.
(2) El-Aneed, A.; Cohen, A.; Banoub, J. *Appl. Spectrosc. Rev.* **2009**, *3*, 210−230.
(3) Tanaka, K. *Angew. Chem., Int. Ed.* **2003**, *33*, 3860−3870.
(4) Karas, M.; Krüger, R. *Chem. Rev.* **2003**, *2*, 427−440.
(5) Pilolli, R.; Palmisano, F.; Cioffi, N. *Anal. Bioanal. Chem.* **2012**, 1−23.
(6) McLean, J. A.; Stumpo, K. A.; Russell, D. H. *J. Am. Chem. Soc.* **2005**, *15*, 5304−5305.
(7) Nizioł, J.; Rode, W.; Zieliński, Z.; Ruman, T. *Int. J. Mass Spectrom.* **2013**, 22−32.

(8) Chiang, C.; Chen, W.; Chang, H. *Chem. Soc. Rev.* **2011**, *3*, 1269−1281.
(9) Castellana, E. T.; Russell, D. H. *Nano Lett.* **2007**, *10*, 3023−3025.
(10) Stumpo, K. A.; Russell, D. H. *J. Phys. Chem. C* **2009**, *5*, 1641−1647.
(11) Amendola, V.; Meneghetti, M. *J. Phys. Chem. C* **2009**, *11*, 4277−4285.
(12) Kreibig, U.; Vollmer, M. *Optical Properties of Metal Clusters*; Springer: Berlin, 1995; .
(13) Cioffi, N.; Colaianni, L.; Pilolli, R.; Calvano, C.; Palmisano, F.; Zambonin, P. *Anal. Bioanal. Chem.* **2009**, *5*, 1375−1383.
(14) Gámez, F.; Hurtado, P.; Castillo, P. M.; Caro, C.; Hortal, A. R.; Zaderenko, P.; Martínez−Haya, B. *Plasmonics* **2010**, *2*, 125−133.
(15) Pilolli, R.; Ditaranto, N.; Di Franco, C.; Palmisano, F.; Cioffi, N. *Anal. Bioanal. Chem.* **2012**, *6−7*, 1703−1711.
(16) Hua, L.; Chen, J.; Ge, L.; Tan, S. N. *J. Nanopart. Res.* **2007**, *6*, 1133−1138.
(17) Daniel, M. C.; Astruc, D. *Chem. Rev.* **2004**, *1*, 293−346.
(18) Amendola, V.; Meneghetti, M. *Phys. Chem. Chem. Phys.* **2009**, *20*, 3805−3821.
(19) Schürenberg, M.; Dreisewerd, K.; Hillenkamp, F. *Anal. Chem.* **1999**, *1*, 221−229.
(20) Lin, P. C.; Tseng, M. C.; Su, A. K.; Chen, Y. J.; Lin, C. C. *Anal. Chem.* **2007**, *9*, 3401−3408.
(21) Vanderpuije, B. N. Y.; Han, G.; Rotello, V. M.; Vachet, R. W. *Anal. Chem.* **2006**, *15*, 5491−5496.
(22) Chiang, N. C.; Chiang, C. K.; Lin, Z. H.; Chiu, T. C.; Chang, H. T. *Rapid Commun. Mass Spectrom.* **2009**, *19*, 3063−3068.
(23) Chiang, C. K.; Lin, Y. W.; Chen, W. T.; Chang, H. T. *Nanomedicine* **2010**, *4*, 530−537.
(24) Huang, Y.; Chang, H. *Anal. Chem.* **2007**, *13*, 4852−4859.
(25) Wu, H. P.; Su, C. L.; Chang, H. C.; Tseng, W. L. *Anal. Chem.* **2007**, *16*, 6215−6221.
(26) Dallaire, A.; Rioux, D.; Rachkov, A.; Patskovsky, S.; Meunier, M. *J. Phys. Chem. C* **2012**, *20*, 11370−11377.
(27) Su, C. L.; Tseng, W. L. *Anal. Chem.* **2007**, *4*, 1626−1633.
(28) Wu, H. P.; Yu, C. J.; Lin, C. Y.; Lin, Y. H.; Tseng, W. L. *J. Am. Soc. Mass Spectrom.* **2009**, *5*, 875−882.
(29) Sherrod, S. D.; Diaz, A. J.; Russell, W. K.; Cremer, P. S.; Russell, D. H. *Anal. Chem.* **2008**, *17*, 6796−6799.
(30) Amendola, V.; Meneghetti, M. *Phys. Chem. Chem. Phys.* **2013**, 3027−3046.
(31) Sajti, C. L.; Sattari, R.; Chichkov, B. N.; Barcikowski, S. *J. Phys. Chem. C* **2010**, *6*, 2421−2427.
(32) Saitow, K.; Okamoto, Y.; Yano, Y. F. *J. Phys. Chem. C* **2012**, *32*, 17252−17258.
(33) Cristoforetti, G.; Pitzalis, E.; Spiniello, R.; Ishak, R.; Giammanco, F.; Muniz-Miranda, M.; Caporali, S. *Appl. Surf. Sci.* **2012**, *7*, 3289−3297.
(34) Tsuji, T.; Mizuki, T.; Yasutomo, M.; Tsuji, M.; Kawasaki, H.; Yonezawa, T.; Mafuné, F. *Appl. Surf. Sci.* **2011**, *6*, 2046−2050.
(35) Nayak, R.; Knapp, D. R. *Anal. Chem.* **2007**, *13*, 4950−4956.
(36) Wada, Y.; Yanagishita, T.; Masuda, H. *Anal. Chem.* **2007**, *23*, 9122−9127.
(37) Nayak, R.; Liu, J.; Sen, A. K.; Knapp, D. R. *Anal. Chem.* **2008**, *22*, 8840−8844.
(38) Li, Z.; Bohn, P. W.; Sweedler, J. V. *Bioresour. Technol.* **2010**, *14*, 5578−5585.
(39) Yonezawa, T.; Kawasaki, H.; Tarui, A.; Watanabe, T.; Arakawa, R.; Shimada, T.; Mafunè, F. *Anal. Sci.* **2009**, 339−346.
(40) Cueto, M.; Sanz, M.; Oujja, M.; Gámez, F.; Martinez− Haya, B.; Castillejo, M. *J. Phys. Chem. C* **2011**, 22217−22224.
(41) Compagnini, G.; Scalisi, A. A.; Puglisi, O. *J. Appl. Phys.* **2003**, 7874.
(42) Amendola, V.; Mattei, G.; Cusan, C.; Prato, M.; Meneghetti, M. *Synth. Met.* **2005**, *2*, 283−286.
(43) Amendola, V.; Meneghetti, M. *J. Mater. Chem.* **2007**, *44*, 4705−4710.
(44) Amendola, V.; Riello, P.; Polizzi, S.; Fiameni, S.; Innocenti, C.; Sangregorio, C.; Meneghetti, M. *J. Mater. Chem.* **2011**, *46*, 18665−18673.
(45) Muto, H.; Yamada, K.; Miyajima, K.; Mafune, F. *J. Phys. Chem. C* **2007**, *46*, 17221−17226.
(46) Sylvestre, J. P.; Poulin, S.; Kabashin, A. V.; Sacher, E.; Meunier, M.; Luong, J. H. T. *J. Phys. Chem. B* **2004**, 16864−16869.
(47) Bonaccorso, F.; Zerbetto, M.; Ferrari, A. C.; Amendola, V. *J. Phys. Chem. C* **2013**, 13217−13229.
(48) Jacksén, J.; Emmer, Å. *Anal. Biochem.* **2012**, *1*, 18−20.